Corrosion Behavior of 18% Ni M250 Grade Maraging Steel under Weld Aged Condition in Hydrochloric Acid Medium

BS Sanatkumar[1], J Nayak[2], *AN Shetty[1]

[1]Department of Chemistry, National Institute of Technology Karnataka, Surathkal, Srinivasnagar - 575 025, Karnataka, India.

[2]Department of Metallurgical and Materials Engineering, National Institute of Technology Karnataka, Surathkal, Srinivasnagar - 575 025, Karnataka, India.

*Correspondence to: A Nityananda Shetty, nityashreya@gmail.com

Accepted: May 2, 2011; Published: July 30, 2011

Abstract

The corrosion behavior of 18% Ni M250 grade maraging steel under weld aged condition has been investigated in hydrochloric acid medium. The studies were carried out in hydrochloric acid solutions of different concentrations (0.1 M – 2 M) at different temperatures (30 ^{0}C – 60 ^{0}C) by potentiodynamic polarization and electrochemical impedance spectroscopy (EIS) techniques. The results showed that the corrosion rate increased with the increase in temperature and with the increase in the concentration of hydrochloric acid in the corrosion medium. Activation parameters were evaluated using Arrhenius equation and transition state equation. The results from the two techniques are in good agreement. The surface morphology of the corroded specimen was compared with that of the un-corroded one by using scanning electron microscopy (SEM).

Keywords: Maraging steel; corrosion rate; EIS; SEM.

1. Introduction

Metals and alloys are used in variety of activities and applications, and are susceptible to corrosion due to their thermodynamic instability, especially, in an aggressive media. Maraging steel is an alloy, which is one of the commercial forms of iron and is very prone to corrosion particularly in acidic medium [1]. Maraging steel was developed in 1960s for applications requiring ultrahigh strength in combination with good fracture toughness. The alloy is a low carbon steel that classically contain about 18 wt % Ni, substantial amounts of Co and Mo together with small additions of Ti. However, depending on the demands dedicated by the application, the composition of the material can be modified [2]. The high strength of maraging steel is achieved by aging at 480 ^{0}C, where precipitation of intermetallics takes place. They have higher modulus of elasticity and lower thermal expansion coefficient. Another important property is its better thermal conductivity, which reduces surface temperature during thermal loading and lowers thermal stresses [3]. Maraging steels have been extensively used in a variety of applications due to their attractive combination of properties such as high strength, moderate toughness and good weld ability [4]. Due to the low carbon content, maraging steels have good machinability. Its strength and malleability allow it to be used in the preparation of rocket and missile skins in aerospace industries, engine components like crankshafts and gears, bearings, submarine hulls, surgical components, nuclear and gas turbine applications [5-8]. For many of the applications of maraging steels, welding is the important means of fabrication. The unique property of being weldable in the solutionized condition followed by a low temperature (480 ^{o}C) post weld maraging treatment makes these steels attractive for fabrication of large structures [9].

According to available literature, atmospheric exposure of 18 Ni maraging steel leads to corrosion in a uniform manner and gets completely rust covered. Pit depths tend to be shallower than in high strength steels [8, 10]. Bellanger et al. [11] have studied the effect of slightly acid pH with or without chloride in radioactive water on the corrosion of maraging steel and have reported that corrosion behavior of maraging steel at the corrosion potential depends on pH and intermediates remaining on maraging steel surface in the active region favoring the passivity. The effect of carbonate ions in slightly alkaline medium on the corrosion of maraging steel was studied by Bellanger [12]. Maraging steels were found to be less susceptible to hydrogen embrittlement than common high strength steels owing to significantly low diffusion of hydrogen in them [13].

Maraging steels come in contact with acids during pickling, acid cleaning, acid descaling, acidizing, etc. But no literature seems to be available which reveals corrosion behavior of 18% Ni M250 grade maraging steel under weld-aged conditions in hydrochloric acid medium. So it is intended to study the corrosion behavior of weld aged maraging steel in hydrochloric acid medium.

2. Methods

2.1. Material

The experiments were performed with specimen of weld-aged maraging steel (18% Ni M250 grade). Percentage composition of 18% Ni M250 grade maraging steel sample is given in Table 1. The weld specimens were taken from the all weld regions of the weld maraging steel. The maraging steel plates of composition as mentioned in Table 1 were welded by gas tungsten arc welding (GTAW) technique using a direct current straight polarity (DCSP), with 5 passes using filler material of composition as given in Table 2.

Table 1: Composition of the specimen (% by weight).

Element	Composition	Element	Composition
C	0.015%	Ti	0.3-0.6%
Ni	17-19%	Al	0.005-0.15%
Mo	4.6-5.2%	Mn	0.1%
Co	7-8.5%	P	0.01%
Si	0.1%	S	0.01%
O	30 ppm	N	30 ppm
H	2.0 ppm	Fe	Balance

Table 2: Composition of the filler material used for welding (% by weight).

Element	Composition	Element	Composition
C	0.015%	Ti	0.015%
Ni	17%	Al	0.4%
Mo	2.55%	Mn	0.1%
Co	12%	Si	0.1%
Fe	Balance		

The specimen was taken from the plates which were welded as per above and aged at 480 ± 5^0 C for three hours followed by air cooling.

2.2. Preparation of test coupons

Cylindrical test coupons were cut from the plate and sealed with epoxy resin in such a way that, the area exposed to the medium was 0.64 cm^2. These coupons were polished as per standard metallographic practice, belt grinding followed by polishing on emery papers, finally on polishing wheel using legated alumina to obtain mirror finish, degreased with acetone, washed with double distilled water and dried before immersing in the corrosion medium.

2.3. Medium

Standard solutions of hydrochloric acid having concentration 0.1 M, 0.5 M, 1 M, 1.5 M and 2 M were prepared by diluting analytical grade hydrochloric acid with double distilled water. Experiments were carried out using calibrated thermostat at temperatures 30 ^{0}C, 40 ^{0}C, 50 ^{0}C and 60 ^{0}C (±0.5 ^{0}C).

2.4. Electrochemical measurements

Electrochemical measurements were carried out by using an electrochemical work station, Gill AC having ACM instrument Version 5 software. A three electrode compartment cell was used for the electrochemical

measurements. The working electrode was made of weld aged maraging steel. A saturated calomel electrode (SCE) and a platinum electrode were used as the reference and the counter electrode, respectively. Electrode potentials were measured with respect to SCE. The polarization studies were done immediately after the EIS studies on the same electrode without any further surface treatment.

2.4.1. Tafel polarization studies

Finely polished weld aged maraging steel specimen of 0.64 cm^2 surface area was exposed to the corrosion medium of different concentrations of hydrochloric acid (0.1 M to 2 M) at different temperatures (30^0C - 60^0C) and allowed to establish a steady state open circuit potential (OCP). The potentiodynamic current potential curves were recorded by polarizing the specimen to -250 mV cathodically and +250 mV anodically with respect to OCP at a scan rate of 1 mV s^{-1}.

2.4.2. Electrochemical impedance spectroscopy studies (EIS)

The corrosion behavior of the specimen was also obtained from EIS technique. In EIS technique, a small amplitude ac signal of 10 mV was applied to the electrochemical system over a wide range of frequencies (10 kHz to 0.01 Hz) at the OCP and the response to the input signal was measured. The charge transfer resistance (R_{ct}) was extracted from the diameter of the semicircle in the Nyquist plot. In all the above measurements, at least three similar results were considered, and their average values are reported.

2.4.3. Scanning electron microscopy (SEM)

The surface morphology of the weld aged maraging steel specimen immersed in HCl solutions were compared with that of the uncorroded one by recording the SEM images of the surfaces using JEOL JSM-6380LA analytical scanning electron microscope. The SEM images were recorded without any gold coating, 20 kV accelerating voltage with 58 μm spot size, under 10^{-7} torr vacuum.

3. Results and Discussion

3.1. Tafel polarization measurement

The effect of hydrochloric acid concentration on the corrosion rate of weld aged samples of maraging steel was studied using Tafel polarization technique. Figure 1 represents potentiodynamic polarization curves for the corrosion of weld aged maraging steel in different concentrations of HCl at 50 ^{0}C. Similar plots were obtained at other temperatures also. It is seen from the figure that the polarization curves are shifted to the high current density region as the concentration of HCl is increased, indicating the increase in the corrosion rate with the increase in HCl concentration. The potentiodynamic polarization parameters like corrosion potential (E_{corr}), corrosion current (i_{corr}), anodic and cathodic slopes (b_a and b_c) and corrosion rate (υ_{corr}) are calculated from Tafel plots and are tabulated in Table 3.

The corrosion rate is calculated using Equation 1.

$$\upsilon_{corr}\ (mmy^{-1}) = \frac{3270 \times M \times i_{corr}}{\rho \times Z} \qquad (1)$$

where 3270 is a constant that defines the unit of corrosion rate, i_{corr} is the corrosion current density in A cm^{-2}, ρ is the density of the corroding material, 8.23 g cm^{-3}, M is the atomic mass of the metal, and Z is the number of electrons transferred per metal atom [14].

It is clear from the data presented in Table 3 that the corrosion rate of weld aged maraging steel specimen increases with increase in the concentration of hydrochloric acid in the solution. It is also observed from the results that the corrosion potential is shifted towards less negative values as the concentration of hydrochloric acid is increased.

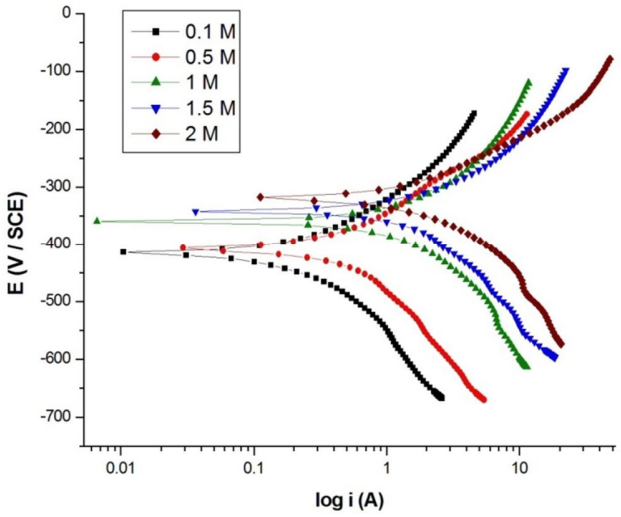

Figure 1: Potentiodynamic polarization curves for the corrosion of weld aged maraging steel in different concentrations of HCl at 50 ^{0}C.

Table 3: Electrochemical polarization parameters for the corrosion of weld aged maraging steel in different concentrations of HCl at different temperatures.

Molarity of HCl	Temperature (K)	E_{corr} (mV vs SCE)	b_a (mV dec^{-1})	$-b_c$ (mV dec^{-1})	i_{corr} (mA cm^{-2})	υ_{corr} (mm y^{-1})
0.1 M	303	-419	170	243	0.22	2.59
	313	-417	172	275	0.30	3.46
	323	-416	174	277	0.31	3.57
	333	-415	175	281	0.32	3.71
0.5 M	303	-413	156	227	0.27	3.05
	313	-414	173	267	0.39	4.58
	323	-413	172	264	0.56	6.45
	333	-411	194	324	1.03	11.87
1 M	303	-371	98	215	0.28	3.94
	313	-363	166	236	0.54	6.27
	323	-359	197	245	0.92	12.74
	333	-358	242	292	1.80	24.73
1.5 M	303	-342	100	223	0.70	8.04
	313	-343	125	235	0.94	12.94
	323	-341	145	239	1.61	22.18
	333	-340	246	333	3.81	43.80
2 M	303	-324	175	287	2.76	31.00
	313	-321	192	325	3.39	39.00
	323	-319	184	340	3.73	42.00
	333	-314	188	337	4.99	57.00

The positive shift in the corrosion potential (E_{corr}) indicates that the anodic process is much more affected by the acid concentration than the cathodic process [15, 16].

The corrosion of steel normally proceeds via two partial reactions in acid solutions. The partial anodic reaction involves the oxidation of metal and formation of soluble Fe^{2+} ions, while the partial cathodic reaction involves the evolution of hydrogen gas [17]. A familiar case is that of placing pure iron in hydrochloric acid. The chemical reaction can be expressed as follows [18].

$$Fe = Fe^{2+} + 2e^{-} \quad (2)$$

$$2H^{+} + 2e^{-} \rightarrow H_2 \uparrow \quad (3)$$

The overall chemical reaction is the sum of these two half-cell reactions:

$$Fe + 2H^{+} \rightarrow Fe^{2+} + H_2 \uparrow \quad (4)$$

3.2. Electrochemical impedance spectroscopy

The corrosion behavior of weld aged sample of maraging steel specimen was also investigated by EIS method in different concentrations of hydrochloric acid at different temperatures. The impedance spectra recorded are displayed as Nyquist plots for the specimen. Figure 2 represents Nyquist plots for the corrosion of weld aged maraging steel in different concentrations of HCl at 50 ^{0}C. Similar plots were obtained at other temperatures also. The point where the semi-circle of the Nyquist plot intersects the real axis at high frequency (close to the origin) yields solution resistance (R_s). The intercept on real axis at the other end of the semicircle (low frequency) gives the sum of solution resistance and the charge transfer resistance (R_{ct}). Hence the charge transfer resistance value is simply the diameter of the semicircle [19]. The diagonal region in between the high frequency and low frequency region has a negative slope due to the capacitive behavior of the electrochemical double layer. R_{ct} is inversely proportional to the corrosion current and was used to calculate the corrosion rate.

The corrosion current density is calculated using the Stern Geary equation (5) [20]:

$$i_{corr} = \frac{b_a b_c}{2.303(b_a + b_c)R_{ct}} \quad (5)$$

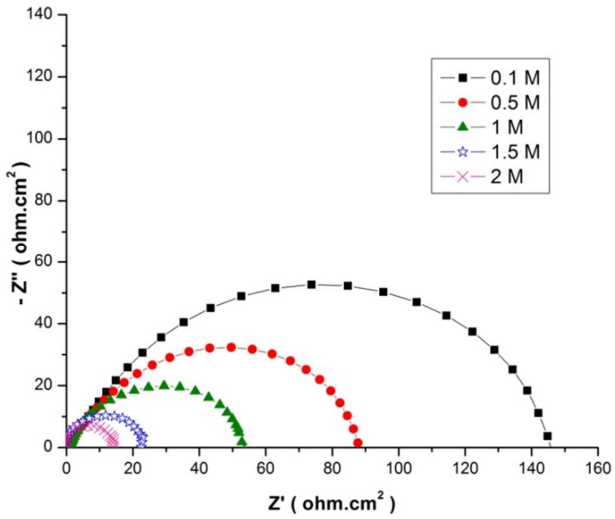

Figure 2: Nyquist plots for the corrosion of weld aged maraging steel in different concentrations of HCl at 50^0 C.

From Figure 2 it is clear that the diameter of the semicircle decreases with the increase in the concentration of HCl, indicating the decrease in R_{ct} value and increase in corrosion rate. The fact that impedance diagrams have semicircular appearance shows that the corrosion of weld aged maraging steel is controlled by a charge transfer process and the mechanism of dissolution of metal in HCl is not altered with the change in the HCl concentration [21]. As seen from the figure, the Nyquist plots are not perfect semicircles. The deviation has been attributed to frequency dispersion. The "depressed" semicircles have a center under the real axis, and can be seen as depressed capacitive loops. Such phenomena often correspond to surface heterogeneity which may be the result of surface roughness, dislocations, distribution of the active sites or adsorption of molecules [22].

The results obtained can be interpreted in terms of the equivalent circuit of the electrical double layer shown in Figure 3 [19]. The circuit fitment was done by ZSimpWin software of version 3.21. It is apparent that all Nyquist plots show a single capacitive loop, in all solutions. The impedance data of weld aged maraging steel in 1 M HCl were analyzed using the circuit fitment shown in Figure 3 in which R_s represents the solution resistance, R_{ct} the charge transfer resistance. The constant phase element (Q_{dl}) is substituted for the capacitive element to give a more accurate fit, as most capacitive loops are depressed semi circles rather than regular semi circles [23].

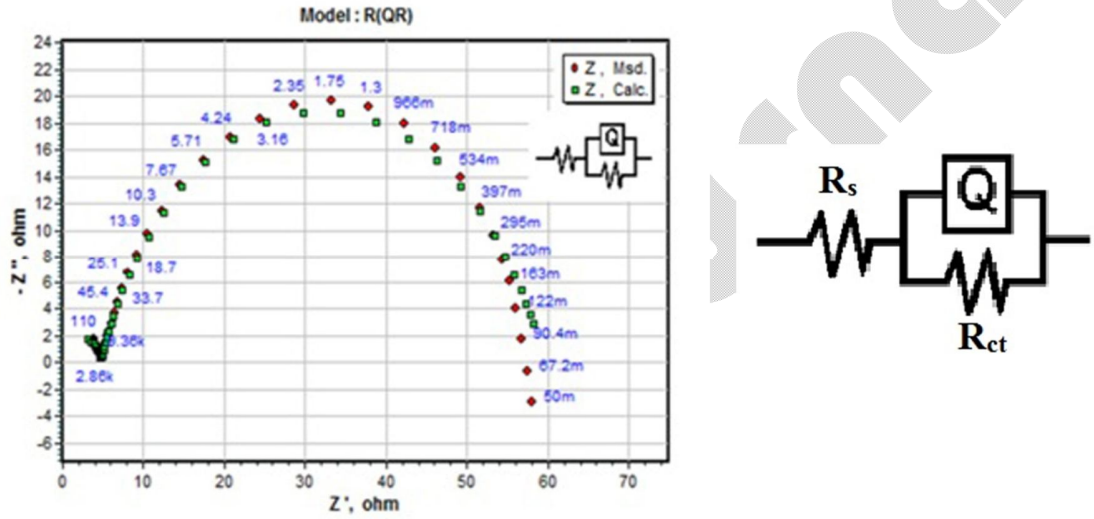

Figure 3: The equivalent circuit model used to fit the experimental data for the corrosion of the specimen in 0.1 M HCl solution at 50^0 C.

The impedance of constant phase is described by the expression:

$$Z_Q = Y_0^{-1}\left(j\omega\right)^{-n} \quad (6)$$

where Y_0 is a proportional factor, n has the meaning of a phase shift and $j = (-1)^{1/2}$. The value of double layer capacitance (C_{dl}) can be obtained from the equation.

$$C_{dl} = Y_0\left(\omega_m^n\right)^{n-1} \quad (7)$$

where ω_m^n is the frequency at which the imaginary part of the impedance has maximum [23]. The results of EIS measurement are summarized in Table 4.

The results show that charge transfer resistance (R_{ct}) value decreases and double layer capacitance (C_{dl}) increases with the increase in the concentration of hydrochloric acid. The increase in the C_{dl} value may be due to desorption of the chloride ions at the metal surface causing a change in the double layer structure [24]. The Nyquist plots

obtained in the real system represent general behavior where the double layer on the interface of metal/solution does not behave as a real capacitor. On the metal side electrons control the charge distribution whereas on the solution side it is controlled by ions. As ions are much larger than the electrons, the equivalent ions to the charge on the metal, will occupy quite a large volume on the solution side of the double layer. Increase in the capacitance, which can result from an increase in local dielectric constant and/or a decrease in the thickness of the electrical double layer, suggests that the chloride molecules act by adsorption at the metal/solution interface [25].

Table 4: Impedance parameters for the corrosion of weld aged maraging steel in different concentrations of HCl at different temperatures.

Concentration	Temperature (K)	C_{dl} ($\mu F\ cm^2$)	R_{ct} ($\Omega\ cm^2$)	υ_{corr} ($mm\ y^{-1}$)
0.1M	303	849	210	2.83
	313	1041	165	3.81
	323	1158	160	3.97
	333	1713	155	4.01
0.5M	303	1057	156	3.54
	313	1133	126	4.87
	323	1733	90	6.88
	333	1857	61	11.83
1M	303	1689	110	3.63
	313	1704	85	6.81
	323	2604	55	11.80
	333	6024	35	22.48
1.5M	303	3028	50	8.21
	313	4049	43	11.28
	323	4516	25	21.47
	333	6567	20	42.00
2M	303	5750	20	32.00
	313	13220	18	40.00
	323	16370	15	44.00
	333	17360	13	55.21

3.3. Effect of temperature

The effect of temperature on the corrosion rate of weld aged maraging steel was studied by measuring the corrosion rate at different temperature between 30^0C – 60^0C. Figures 4 and 5 represent the potentiodynamic polarization curves and Nyquist plots, respectively, at different temperatures for the corrosion of weld aged maraging steel sample in 1 M HCl solution. Similar plots were obtained in other concentrations of solutions also. The Tafel polarization results and EIS results at different temperatures are listed in Tables 3 and 4, respectively. From the Figures 4 and 5 and from the results in Tables 3 and 4 it is seen that the corrosion rate increases with the increase in temperature. This may be attributed to the fact that the hydrogen evolution overpotential decreases with the increase in temperature that leads to the increase in cathodic reaction rate [26]. The values of b_c and b_a change with the increase in acid concentration and also with the increase in temperature, which indicate the influence of acid concentration and temperature on the kinetics of hydrogen evolution and metal dissolution.

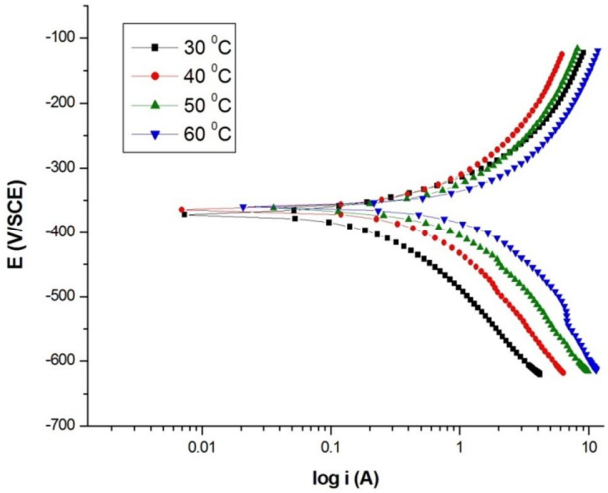

Figure 4: Potentiodynamic polarization curves for the corrosion of weld aged maraging steel in 1 M hydrochloric acid at different temperatures.

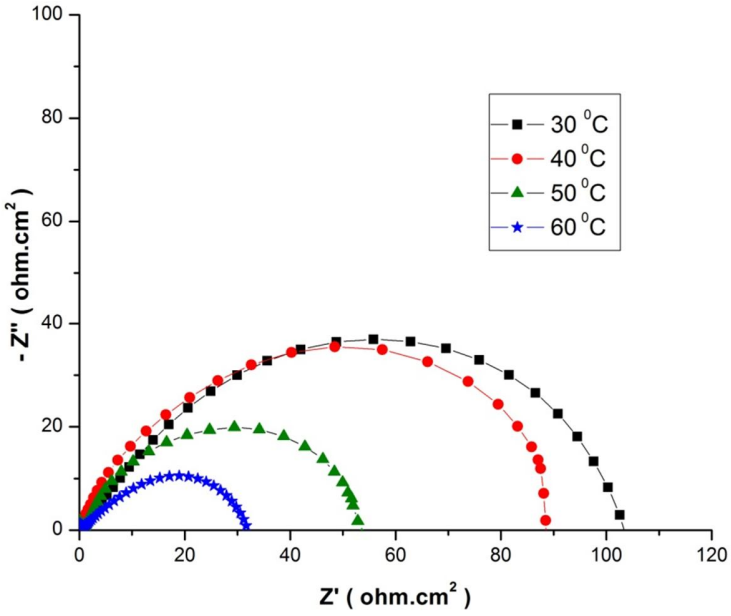

Figure 5: Nyquist plots for the corrosion of weld aged maraging steel in 1 M HCl at different temperatures.

Activation energy (E_a) for the corrosion process of weld aged maraging steel in hydrochloric acid was calculated from the Arrhenius equation (Eq. 8) [8, 10].

$$\ln(\upsilon_{corr}) = B - (E_a / RT) \quad (8)$$

where *B* is a constant which depends on the metal type, and *R* is the universal gas constant. The plot of ln (υ_{corr}) versus reciprocal of absolute temperature (*1/T)* gives a straight line whose slope = $-E_a / R$, from which the activation energy values for the corrosion process were calculated. The Arrhenius plots for the weld aged specimen are shown in Figure 6.

The enthalpy of activation ($\Delta H^{\#}$) and entropy of activation ($\Delta S^{\#}$) values for the corrosion process were calculated from transition state theory Equation 9 [24].

$$\upsilon_{corr} = (RT/Nh) \exp(\Delta S^{\#}/R) \exp(-\Delta H^{\#}/RT) \quad (9)$$

where *h* is Planck's constant, and *N* is Avagadro's number and R is the ideal gas constant. A plot of $\ln(\upsilon_{corr}/T)$ versus *1/T* gives a straight line with slope = $-\Delta H^{\#}/R$ and intercept = $\ln(R/Nh) + \Delta S^{\#}/R$. The plots of $\ln(\upsilon_{corr}/T)$ versus *1/T* for the corrosion of weld aged maraging steel in different concentrations of hydrochloric acid is shown in Figure 7.

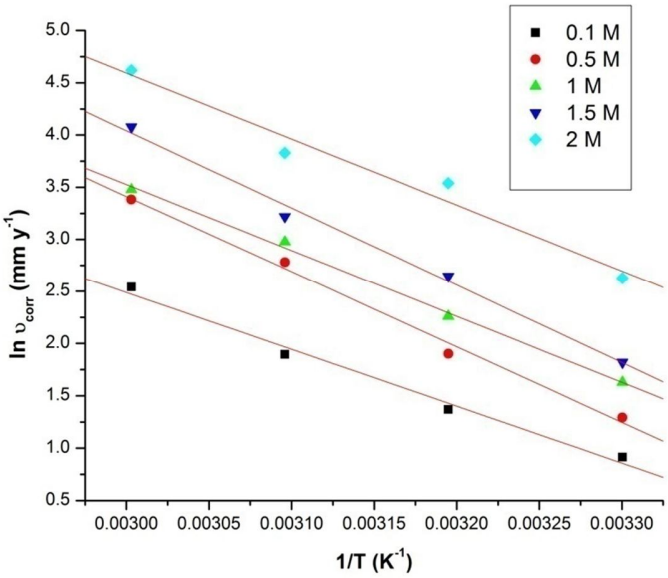

Figure 6: Arrhenius plots for the corrosion of weld aged maraging steel in HCl.

The activation parameters calculated are listed in Table 5. The activation energy values indicate that the corrosion of the alloy is controlled by surface reaction, since the values of activation energy for the corrosion process are greater than 20 kJ mol^{-1} [27]. The entropy of activation is negative. This implies that the activated complex in the rate-determining step represents association rather than dissociation, indicating that a decrease in randomness takes place on going from reactants to the activated complex [25].

3.4. Scanning electron microscopy (SEM)

The scanning electron microscope images were recorded to establish the interaction of acid solution with the metal surface. The SEM image of a freshly polished surface of weld aged maraging steel sample is given in Figure 8a, which shows the uncorroded surface with few scratches due to polishing. Figure 8b shows the SEM image of weld aged maraging steel surface after immersed for 3 h in 2.0 M HCl. The SEM images reveal that the specimen not immersed in the acid solutions is in a better condition having a smooth surface while the metal surface immersed in 2.0 M HCl is deteriorated due to the acid action. The corroded surface shows detachment of particles

from the surface. The corrosion of weld aged alloy may be predominantly attributed to the inter-granular corrosion assisted by the galvanic effect between the precipitates and the matrix along the grain boundaries.

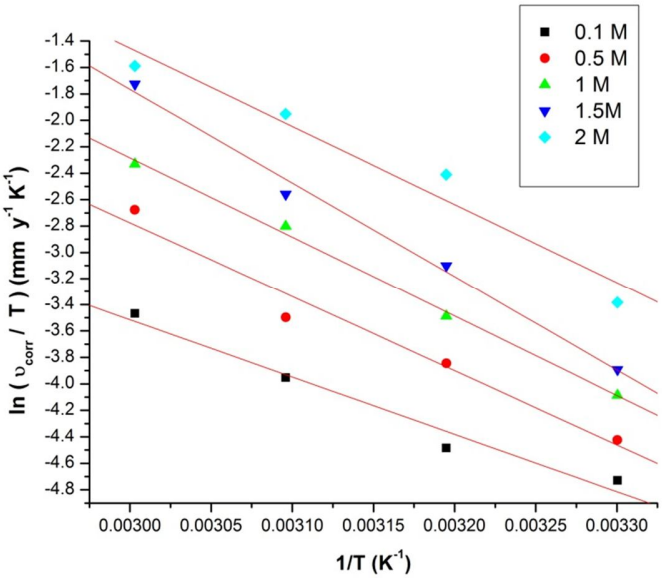

Figure 7: Plots of $\ln(\upsilon_{corr}/T)$ vs 1/T for the corrosion of weld aged maraging steel in HCl.

Table 5: Activation parameters for the corrosion of weld aged maraging steel in hydrochloric acid.

Molarity of HCl	E_a (kJ mol^{-1})	$\Delta H^{\#}$ (kJ mol^{-1})	$\Delta S^{\#}$ (J mol^{-1} K^{-1})
0.1 M	35	34	-114
0.5 M	33	35	-122
1 M	48	49	-81
1.5 M	46	45	-89
2 M	32	33	-116

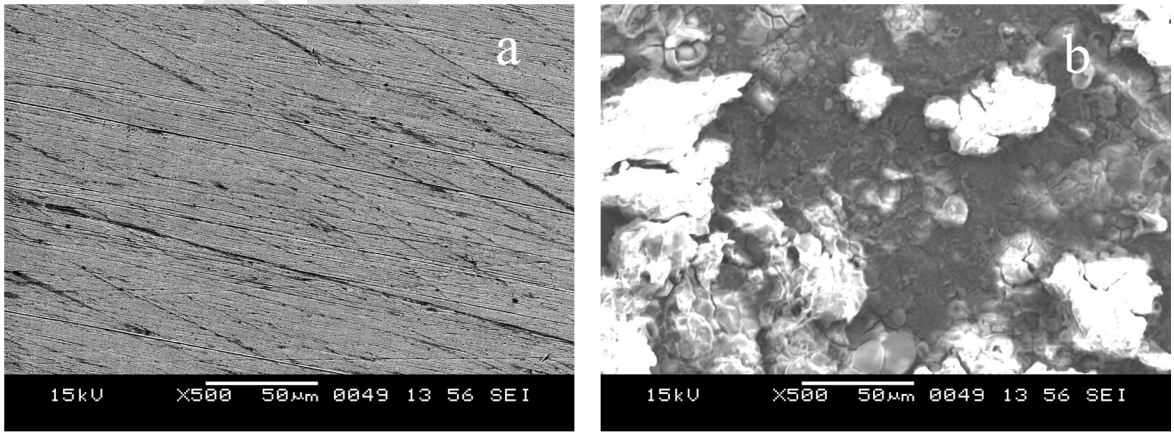

Figure 8: SEM images of (a) Freshly polished surface, (b) Corroded surface.

4. Conclusion

Systematic studies of the corrosion behavior of the weld aged maraging steel in different concentrations of hydrochloric acid at different temperatures by electrochemical methods lead to the following conclusions.
1. The corrosion rate of weld aged maraging steel specimen in hydrochloric acid medium is substantial.
2. The potentiodynamic polarization and impedance studies showed that the corrosion rate of the specimen is influenced by temperature and concentration of hydrochloric acid medium. The corrosion rate increases with the increase in the concentration of hydrochloric acid and solution temperature.
3. The corrosion rate determined by potentiodynamic polarization and EIS are in reasonably good agreement.
4. The corrosion kinetics follows Arrhenius law.

Competing Interests

The authors declare that they have no competing interests.

Authors' Contributions

SBS carried out the experimental work under the guidance of JN and ANS and drafted the manuscript. JN and ANS helped in the interpretation of the results and finalizing the draft.

References

[1] Poornima T, Nayak J, Shetty AN, 2010. Studies on corrosion of annealed and aged 18 Ni 250 grade maraging steel in sulfuric acid medium. Portugaliae Electrochimica Acta, 28: 173-188.

[2] Stiller K, Danoix F, Bostel A, 1996. Investigation of precipitation in a new maraging stainless steel. Applied Surface Science, 94/95: 326-333.

[3] Klobcar D, Tusek J, Taljat B, et al., 2008. Aging of maraging steel welds during aluminum alloy die casting. Materials Science, 44: 515–522.

[4] Grum J, Slabe JM, 2006. Effect of laser-remelting of surface cracks on microstructure and residual stresses in 12Ni maraging steel. Applied Surface Science, 252: 4486–4492.

[5] Razek J, Klein IE, Yahalom J, 1997. Structure and corrosion resistance of oxides grown on maraging steel in steam at elevated temperatures. Applied Surface Science, 108: 159-167.

[6] Ohue Y, Matsumoto K, 2007. Sliding–rolling contact fatigue and wear of maraging steel roller with ion-nitriding and fine particle shot-peening. Wear, 263: 782–789.

[7] Wang W, Yan W, Duan Q, et al., 2010. Study on fatigue property of a new 2.8 GPa grade maraging steel. Materials Science and Engineering, A 527: 3057–3063.

[8] Poornima T, Nayak J, Shetty AN, 2010. Corrosion of aged and annealed 18 Ni 250 grade maraging steel in phosphoric acid medium. International Journal of Electrochemical Science, 5: 56–71.

[9] Adama CM, Travis RE, 1964. Welding of 18% Ni-Co-Mo maraging alloys Welding Journal, 43: 193–197.

[10] Poornima T, Nayak J, Shetty AN, 2011. 3, 4-Dimethoxy benzaldehyde thiosemicarbazone as corrosion inhibitor for aged 18Ni 250 grade maraging steel in 0.5 M sulfuric acid. Journal of Applied Electrochemistry, 41: 223-233.

[11] Bellanger G, Rameau JJ, 1996. Effect of slightly acid pH with or without chloride in radioactive water on the corrosion of maraging steel. Journal of Nuclear Materials, 228: 24.

[12] Bellanger G, 1994. Effect of carbonate in slightly alkaline medium on the corrosion of maraging steel. Journal of Nuclear Materials, 217: 187.

[13] Rezek J, Klein IE, Yhalom J, 1997. Electrochemical properties of protective coatings on maraging steel. Corrosion Science, 39: 385.

[14] Fontana MG, 1987. Corrosion Engineering, 3rd edn. McGraw Hill, Singapore.

[15] Machnikova E, Whitmire HK, Hackerman N, 2008. Corrosion inhibition of carbon steel in hydrochloric acid by furan derivatives. Electrochimica Acta, 53: 6024–6032.

[16] Touhamia F, Aounitia A, Abeda Y, et al., 2000. Corrosion inhibition of armco iron in 1 M HCl media by new bipyrazolic derivatives. Corrosion Science, 42: 929-940.

[17] Kriaa A, Hamdi N, Jbali K, et al., 2009. Corrosion of iron in highly acidic hydro-organic solutions. Corrosion Science, 51: 668–676.

[18] Amin AM, Khaled KF, Mohsen Q, et al., 2010. A study of the inhibition of iron corrosion in HCl solutions by some amino acids. Corrosion Science, 52: 1684–1695.

[19] Prabhu RA, Venkatesha TV, Shanbhag AV, et al., 2008. Inhibition effects of some Schiff's bases on the corrosion of mild steel in hydrochloric acid solution. Corrosion Science, 50: 3356–3362.

[20] El-Sayed A, 1997. Phenothiazine as inhibitor of the corrosion of cadmium in acidic solutions. Journal of Applied Electrochemistry, 27: 94.

[21] Larabi L, Harek Y, Benali O, et al., 2005. Inhibition of the corrosion of iron by oxygen and nitrogen containing compounds. Progress in Organic Coatings, 54: 261.

[22] Li W, He Q , Zhang S , et al., 2008. Some new triazole derivatives as inhibitors for mild steel corrosion in acidic medium. Journal of Applied Electrochemistry, 38: 289–295.

[23] Tang Y, Chen Y, Yang W, et al., 2008. Electrochemical and theoretical studies of thienyl-substituted amino triazoles on corrosion inhibition of copper in 0.5 M H_2SO_4. Journal of Applied Electrochemistry, 38: 1553-1559.

[24] Abd Ei-Rehim SS, Ibrahim MAM, Khaled KF, 1999. 4-Aminoantipyrine as an inhibitor of mild steel corrosion in HCl solution. Journal of Applied Electrochemistry, 29: 595.

[25] Prabhu RA, Shanbhag AV, Venkatesha TV, 2007. Influence of tramadol [2-[(dimethylamino)methyl]-1-(3-methoxyphenyl) cyclohexanol hydrate] on corrosion inhibition of mild steel in acidic media. Journal of Applied Electrochemistry, 37: 491–497.

[26] Larabi L, Harek Y, Benali O, et al., 2005. Hydrazide derivatives as corrosion inhibitors for mildsteel in 1M HCl. Progress in Organic Coatings, 54: 261.

[27] Bouklah M, Hammouti B, Benkaddour M, et al., 2005. Thiophene derivatives as effective inhibitors for the corrosion of steel in 0.5 M H_2SO_4. Journal of Applied Electrochemistry. 35: 1095–1101.